Available online at www.sciencedirect.com

SCIENCE DIRECT

Developmental Biology 276 (2004) 207–224

DEVELOPMENTAL BIOLOGY

www.elsevier.com/locate/ydbio

A new origin for the maxillary jaw

Sang-Hwy Lee[a], Olivier Bédard[b,1], Marcela Buchtová[b], Katherine Fu[b], Joy M. Richman[b,*]

[a]*Department of Oral, Maxillofacial Surgery and Oral Science Research Center, Medical Science and Engineering Research Center, BK 21 Project for Medical Science, College of Dentistry Yonsei University, Seoul, Korea*

[b]*Department of Oral Health Sciences, Faculty of Dentistry, University of British Columbia, Vancouver, BC, Canada, V6T 1Z3*

Received for publication 7 April 2004, revised 5 August 2004, accepted 31 August 2004
Available online 5 October 2004

Abstract

One conserved feature of craniofacial development is that the first pharyngeal arch has two components, the maxillary and mandibular, which then form the upper and lower jaws, respectively. However, until now, there have been no tests of whether the maxillary cells originate entirely within the first pharyngeal arch or whether they originate in a separate condensation, cranial to the first arch. We therefore constructed a fate map of the pharyngeal arches and environs with a series of dye injections into stage 13–17 chicken embryos. We found that from the earliest stage examined, the major contribution to the maxillary bud is from post-optic mesenchyme with a relatively minor contribution from the maxillo-mandibular cleft. Cells labeled within the first pharyngeal arch contributed exclusively to the mandibular prominence. Gene expression data showed that there were different molecular codes for the cranial and caudal maxillary prominence. Two of the genes examined, *Rarβ* (*retinoic acid receptor β*) and *Bmp4* (bone morphogenetic protein) were expressed in the post-optic mesenchyme and epithelium prior to formation of the maxillary prominence and then were restricted to the cranial half of the maxillary prominence. In order to determine the derivatives of the maxillary prominence, we performed focal injections of CM-DiI into the stage 24 maxillary prominence. Labeled cells contributed to the maxillary, palatine, and jugal bones, but not the other elements of the upper beak, the premaxilla and prenasal cartilage. We also determined that the cranial cells give rise to more distal parts of the upper beak, whereas caudal cells form proximal structures. Grafts of stage 24 maxillary prominences were also analyzed to determine skeletal derivatives and these results concurred with the DiI maps. These early and later fate maps indicate that the maxillary prominence and its skeletal derivatives are not derived from the first pharyngeal arch but rather from a separate maxillary condensation that occurs between the eye and the maxillo-mandibular cleft. These data also suggest that during evolution, recession of the first pharyngeal arch-derived palatoquadrate cartilage to a more proximal position gave way to the bony upper jaw of amniotes.

Keywords: Fate mapping; Craniofacial; Maxilla; Palatine bone; Jugal; Quadratojugal; Palate; Facial prominence; Mandibular arch; First pharyngeal arch; Visceral arch; Trabeculae cranii; *Rarβ*; Bone morphogenetic protein; Retinoic acid; Dye labeling

Introduction

The commonly held view is that the first and most cranial pharyngeal arch, the mandibular arch, subdivides to form the maxillary and mandibular facial prominences during embryogenesis from which the maxillary and mandibular jaws develop (Moore and Persaud, 2003; Sperber, 2001). The second pharyngeal arch also has specialized derivatives including the tongue musculature and the skeletal elements supporting the tongue in some vertebrates. The more caudal branchial arches are less specialized and are more homologous to the repeating segmented arches of primitive vertebrates. Since the first and second arch have unique characteristics, they are best not referred to as branchial arches (Nelson, 1953). Other tissue buds or prominences of the face form cranial to the first arch including the lateral nasal (lateral to the nasal pits) and the medial nasal (between

* Corresponding author. Department of Oral Health Sciences, Faculty of Dentistry, University of British Columbia, 2199 Wesbrook Mall, Vancouver, BC, Canada, V6T 1Z3. Fax: +1 604 822 3562.
E-mail address: richman@interchange.ubc.ca (J.M. Richman).
[1] Present address: Faculté de Médecine Dentaire de l'Université Laval, Québec City, QC, Canada G1K 7P4.

0012-1606/$ - see front matter © 2004 Elsevier Inc. All rights reserved.
doi:10.1016/j.ydbio.2004.08.045

the nasal pits). The maxillary prominences are the last to form and they flank the sides of the stomodeum (Yee and Abbott, 1978). This arrangement of facial prominences is characteristic of higher vertebrates including mammals, aves, and reptiles (Haeckel, 1886). The upper jaw, the focus of our study, is formed as a result of the fusion and merging of the medial nasal, lateral nasal, and maxillary prominences.

The neural crest from the caudal mesencephalon and cranial hindbrain (rhombomere 1; Kontges and Lumsden, 1996) together contribute to the first pharyngeal arch and other more cranial parts of the head such as the mesenchyme between the eye and the maxillo-mandibular cleft (post-optic). When quail-chicken chimeras are allowed to develop until the skull has formed, most of the mandibular bones, maxillary, palatine, jugal, and the jugal process of the quadratojugal bone share a common origin in the caudal mesencephalon (Kontges and Lumsden, 1996). These data do not allow us to determine the precise origins of maxillary and mandibular regions. What is necessary is a map that begins just at the time when the first visceral arch forms or in other words at the end of active neural crest cell migration.

The evolutionary significance of this question relates to how the jaws evolved from their most primitive state in agnathans such as lamprey to the mammalian form. The upper jaw of birds, reptiles and mammals has diverged considerably from that of amphibians and fishes and the embryonic basis for this difference is not known. Fishes generally form a cartilage element in the maxillary jaw, which is continuous with a proximal quadrate cartilage. The entire structure is called palatoquadrate due to the large, distally extended pterygoid process. Thus the upper jaw is initially supported by a cartilage rod similar to Meckel's cartilage in the mandibular arch (de Beer, 1937; Janvier, 1996). External to this cartilage form a series of dermal bones (plates) and these reinforce the upper jaw (Cubbage and Mabee, 1996). In contrast, birds and reptiles do not form a cartilaginous skeletal element in the upper jaw but instead form a more proximally located quadrate that lacks the exaggerated pterygoid process and contributes only to the joint. In all amniotes, a series of separate intramembranous bones including the palatine, maxillary, jugal, and quadratojugal condense to form the main support for the upper jaw. Amphibians also have membranous bone supporting the upper jaw; however, the bones are somewhat reduced in size and different in morphology (Janvier, 1996). In bony fish, although analogous dermal bones are present, such as the maxillary and premaxillary, they are in a completely different position and do not serve to close the roof of the oral cavity. One possible scenario that would account for the apparent lack of functional homology between the maxillary bones of amniotes and bony fishes may be differences in the embryonic rudiment from which they derive.

It is important to understand more about the fate of the first pharyngeal arch so that we can better interpret craniofacial phenotypes in humans and in animal models. Currently, there is a general view that all maxillary bones should be assigned to the first pharyngeal arch (see, for example, Smith and Schneider, 1998), even though there is no experimental proof that this is correct. We wished to resolve whether cells are segregated into a cranial maxillary condensation and caudal mandibular condensation from the earliest stages of pharyngeal arch formation or whether cells derived from the first pharyngeal arch contribute to the maxillary region, thereby forming the maxillary process (Richman and Lee, 2003). In this study, we use the avian embryo, which has a distinct maxillary bud to map the fate of the first pharyngeal arch. We begin our mapping during stages of early pharyngeal arch formation (stage 13; Hamburger and Hamilton, 1951) and on into facial prominence formation (stage 24). Our dye maps clearly show that the first pharyngeal arch mesenchyme does not give rise to most of the maxillary process and that there is a unique origin for this region. Furthermore, the dye labeling and gene expression patterns suggest that there may be a cranial to caudal gradient first in the maxillary condensation and later in the maxillary prominence that is interpreted to generate distal to proximal skeletal patterning in the upper jaw.

Materials and methods

Chick embryos

Fertilized White Leghorn chicken eggs were obtained from Choonang animal disease laboratory (Daejeon, Korea) or the University of Alberta (Edmonton, AB). Eggs were incubated at 38°C and staged according to Hamburger and Hamilton (H–H; 1951).

DiI labeling of embryos

We selected dye labeling methods over retroviral or quail transplants in order to track groups of neural crest derived mesenchymal cells through facial development. For the purposes of our study, it was not essential to permanently label or to label all cells. The idea was to use a noninvasive method that would permit normal development to identify the region that mesenchymal cells from a particular domain contribute. We injected the DiI (1,1′ -dioctadecyl-3,3,3′ ,3′ -tetramethylindocarbocyanine perchlorate, Molecular Probes Inc., OR, USA) into the face (N = 288) of stage 13–17 embryos with picospritzer II (General Valve Co., NJ, USA). During the injection procedure, a bit of epithelium at the injection point was elevated for easy injection as well as to limit the dye to the mesenchyme rather than epithelium. The epithelium regrows rapidly and no defects in the face are produced by this procedure. Instead of using absolute measurements, we located the injection sites according to anatomical landmarks (Figs. 1A–C). This made it possible

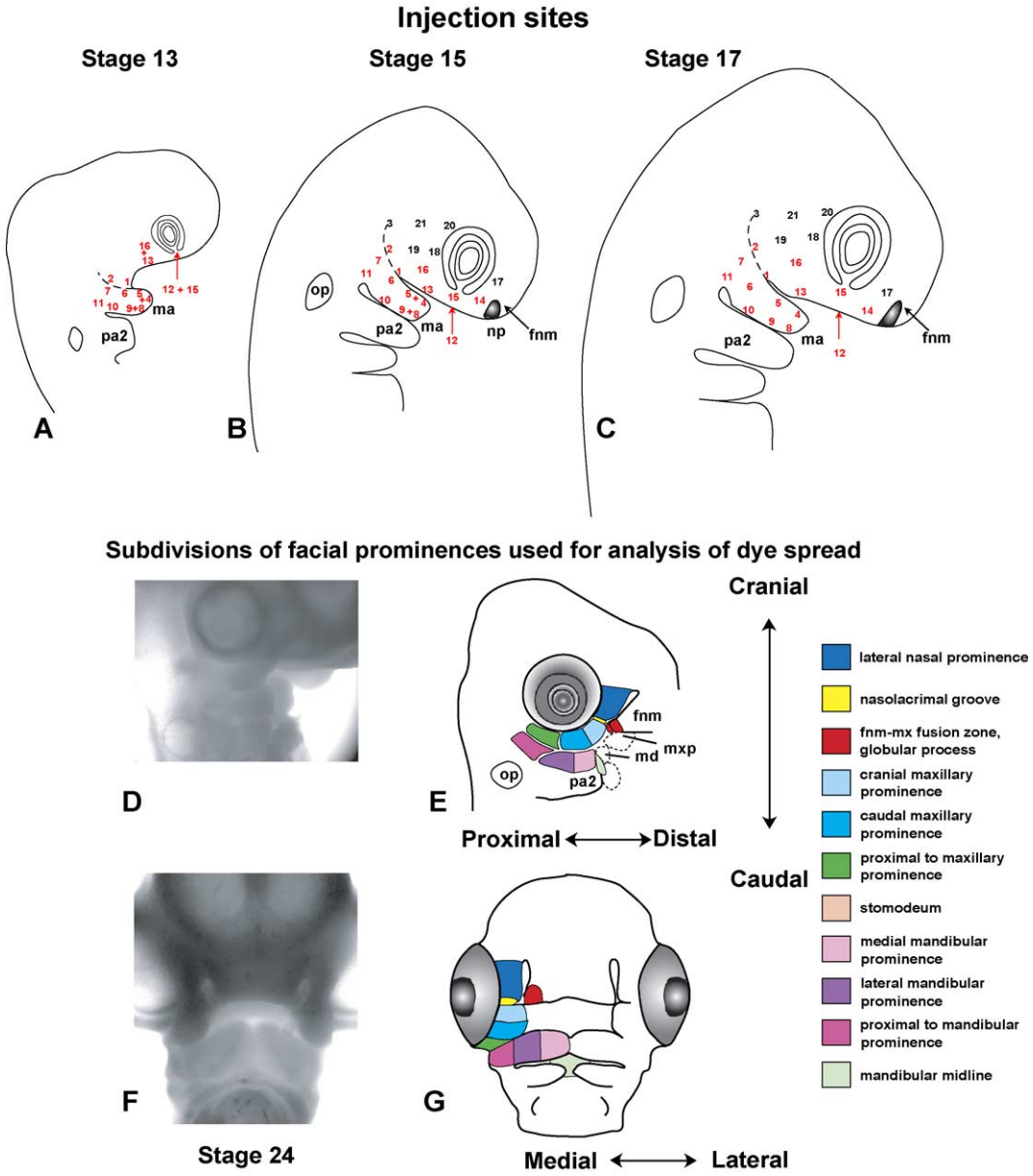

Fig. 1. Positions of dye injections in different staged chicken embryos and map of dye spread in the stage 24 embryo. Numbers in red indicate sites that contributed to the face. Numbers in black did not contribute to the facial prominences. (A, B, C) Lateral drawings of the external surface of different staged chicken embryos. Several sites were combined in stages 13 and 15 embryos due to the small size. Post-optic region includes sites 13 and 16. (D, E) Three quarters view of the stage 24 face, 48 h after the injections was performed. Arbitrary divisions of the facial prominences are indicated. The spread of dye into each region was noted from lateral and frontal positions according to the axes indicated. (F, G) Frontal view of stage 24 embryo showing the additional areas that could be labeled with dye. Key: fnm—frontonasal mass, ma—mandibular arch or first pharyngeal arch, md—mandibular prominence, mxp—maxillary prominence, np—nasal pit, op—otic pit, pa2—second pharyngeal arch.

to use anatomically equivalent sites in different stages embryos. Due to the smaller size of the stage 13 embryo, there were fewer sites injected at these stages than at stage 15 or 17. Embryos were labeled with a few drops of the vital dye Neutral Red (Fisher Sci.) in order to stain the somites (for accurate staging), resolve the pharyngeal arches, and to see the nasal placode. This dye does not affect development.

Simultaneous injections of DiI and DiO (3,3′-dioctadecyloxacarbocyanine perchlorate, Molecular Probes) were done in a subset of embryos and examined with a BioRad Radiance confocal microscope to confirm the extent of mixing of adjacent cell groups.

After the single or double injection, the embryos were incubated for 48 h to reach stage 22–25, all are stages when there are distinct maxillary and mandibular prominences. Embryos were harvested and fixed in 4% paraformaldehyde with 0.25% glutaraldehyde. A subset of embryos were embedded in OCT, sectioned with a cryostat in order to reveal the extent of mesenchymal labeling, which is not

always easy to appreciate with whole embryos. Sections were counterstained with hematoxylin and eosin.

To extend our fate maps to stages when bone had developed, we injected stage 24 maxillary prominences with fixable dye (CM-DiI, Molecular Probes). The crystals were dissolved in dimethyl sulfoxide (DMSO) and diluted to a working concentration of 0.5 mg/ml in 0.3 M sucrose. Dye was injected into the right maxillary prominence in one of three positions (1) cranial edge, (2) caudal edge, (3) multiple positions. At 3–6 h postinjection, pictures were taken in ovo with a MZFLIII Leica fluorescence stereo microscope (Rhodamine filter set) and monochrome camera (QiCam, Qimaging, Burnaby) to evaluate the position of the fluorescent labeling. The specimens where the dye had not remained in the original injection site were not considered in the data analysis. Embryos were sacrificed at stage 34, fixed in 10% formaldehyde with 5.5% EDTA, pH 7.0. The lower beaks and tongues were removed and photographs were taken of the palate under fluorescence illumination.

Analysis of dye spread in embryos injected at stages 13–17 and fixed at stage 24

After reviewing the images, we divided the stage 24 chick embryonic face including maxillo-mandibular regions according to anatomy and to give some finer resolution to the DiI fate map, as shown in Figs. 1E,G. Scoring for presence of label was done in the following manner: Areas with less than five cells labeled were scored as having no label, areas with five or more cells label were scored as having label, qualitative data on the degree of expansion of the label within a compartment was combined with signal intensity and assigned an arbitrary score out of 3 where 1 was the least bright and 3 was the brightest (Table 1A–C).

Dye spread analysis of embryos injected at stage 24 and fixed at stage 34

The palate was divided into 7 arbitrary regions where 1 was the most distal and 6, 7 were the most proximal. Photographs of the palate were analyzed and each specimen was classified according to regions that were labeled with dye (Table 2).

For histological analysis, embryos remained in the decalcifying solution for at least 1 week, the eyes were removed for a better penetration of the tissue and then a subset of embryos was embedded in wax (n = 4) or in 20% gelatin (n = 12). Those that were representative of the general pattern of macroscopic dye spread for each of the three injection sites were selected for histological examination. The specimens were sectioned in a frontal plane from the tip of the beak to the pharynx. Gelatin sections (80–150 μm) were obtained with an EMS Vibratome, floated onto chromium–alum subbed slides, and coverslipped with 10% PBS/glycerol. Paraffin sections (5–7 μm) were laid on noncoated glass slides. Alternate sections were left unstained or were stained with a combination of Picosirius Red and Alcian blue (Ashique et al., 2002b). This stain highlights bone as red and cartilage as blue but is incompatible with fluorescence emission. Unstained sections were examined with a Zeiss compound fluorescence microscope under Rhodamine excitation. Positions of bones in unstained sections were determined by comparison to adjacent, stained sections. Each section was scored for presence or absence of dye in the maxillary, jugal, and palatine bones (Table 2).

In situ hybridization

In situ hybridization was performed in whole mount with an In Situ Pro robot, (INTAVIS Bioanalytical Instruments AG) using protocols previously described (Shen et al., 1997). Chicken probes were generously provided by the following individuals: *Fgf-8*, J.C. Ispizúa Belmonte; *Msx1*, S. Wedden; *Barx1*, *Bmp4*, P. Francis-West; *Rarβ*, P. Brickell.

Grafts of stage 24 maxillary prominences

Stage 24 maxillary prominences were either removed whole or bisected into cranial and caudal halves. Prominences were collected in Hanks buffered salt solution with 10% fetal calf serum on ice. To prepare the host graft site, a square of tissue (epithelium and mesenchyme) roughly 500 μm^2 was removed from the wing buds of host embryos at stage 22–23. Grafts were pinned into position, mesenchymal side down, with L-shaped platinum wire (0.025 mm, Goodfellow). Host embryos were grown for an additional 10 days to ensure grafts developed bone. This graft site has previously been shown to provide a neutral but supportive environment for donor tissue (Richman et al., 1997). Fixation and staining of bone and cartilage in host limbs and grafts was done as described (Plant et al., 2000). Grafts that did not develop bone were eliminated from further analysis. Grafts in which bone had formed were removed from the host limb and each bone within the graft was dissected. Individual bones were analyzed for specific features and identities assigned as indicated in Table 3.

Results

Stage-specific patterns of dye spread

Neural crest cells enter the distal facial prominences and first visceral arch soon after they emigrate. By stage 12, the only cranial neural crest cells that are still emigrating are those in the hindbrain; however, these cells stay mainly proximal to the mandibular arch and more caudal pharyngeal arches (Baker et al., 1997). By the time we inject dye into the embryo at stage 13, the embryo has turned and a distinct mandibular arch has just formed (Shigetani et al., 2000). Even though the initial injection points were of a similar size at stages 13, 15,

Table 1
Location and intensity of dye spread in the stage 24 face from different injection sites

A. Stage 13[a], $N = 59$

Injection site	N	prox to Md	lateral Md	medial Md	prox to Mxp	Post Mxp	Ant Mxp	FMFZ	Nasolacrimal groove	LNP	Md midline	Stomodeum	Globular process
1	5	0	5	3	4	5	1	0	0	0	0	0	0
2	4	2	3	0	3	1	0		0	0	0	0	0
4 + 5	8	0	0	8	0	0	0	0	0	0	7	0	0
6	6	1	3	5	1	0	0	0	0	0	0	0	0
7	6	6	5	1	4	0	0	0	0	0	0	0	0
8 + 9	6	0	5	1	0	0	0	0	0	0	5	0	0
10	3	2	3	3	0	0	0	0	0	0	0	0	0
11	8	7	3	1	6	0	0	0	0	0	0	0	0
12 + 15	6	0	0	0	4	4	3	1	2	0	0	5	0
13 + 16	7	0	0	0	7	6	3	0	0	0	0	0	0

B. Stage 15[a], $N = 144$

Injection site	N	prox to Md	lateral Md	medial Md	prox to Mxp	Post Mxp	Ant Mxp	FMFZ	Nasolacrimal groove	LNP	Md midline	Stomodeum	Globular process
1	26	9	24	4	23	25	2	0	0	0	0	0	0
2	18	3	7	0	17	3	0	0	0	0	0	0	0
4 + 5	7	0	0	7	0	0	0	0	0	0	5	0	0
6	10	0	10	2	1	0	0	0	0	0	0	0	0
7	5	4	5	0	5	0	0	0	0	0	0	0	0
8 + 9	17	0	0	17	0	0	0	0	0	0	13	0	0
10	7	0	7	0	1	0	0	0	0	0	0	0	0
11	7	7	4	0	1	0	0	0	0	0	0	0	0
12	7	0	0	0	0	0	5	7	0	0	0	7	0
13	10	0	0	0	3	1	9	0	0	0	0	6	0
14	9	0	0	0	0	1	2	0	7	8	0	0	2
15	7	0	0	0	0	0	7	5	0	0	0	7	0
16	8	0	0	0	3	8	8	0	0	0	0	0	0
17	6	0	0	0	0	0	0	0	5	6	0	0	0

C. Stage 17[a], $N = 85$

Injection site	N	prox to Md	lateral Md	medial Md	prox to Mxp	Post Mxp	Ant Mxp	FMFZ	Nasolacrimal groove	LNP	Md midline	Stomodeum	Globular process
1	7	0	5	0	5	2	0	0	0	0	0	0	0
2	5	0	4	0	5	0	0	0	0	0	0	0	0
4	5	0	0	5	0	0	0	0	0	0	5	0	0
5	4	0	0	4	0	0	0	0	0	0	0	0	0
6	5	0	5	0	0	0	0	0	0	0	0	0	0
7	10	0	10	0	0	0	0	0	0	0	0	0	0
8	3	0	0	3	0	0	0	0	0	0	2	0	0
9	8	0	3	8	0	0	0	0	0	0	5	0	0
10	7	0	7	2	0	0	0	0	0	0	0	0	0
11	6	6	2	0	0	0	0	0	0	0	0	0	0
12	6	0	0	0	0	1	5	0	1	0	0	5	0
13	3	0	0	0	1	3	2	0	0	0	0	0	0
14	4	0	0	0	0	0	0	1	5	2	0	0	4
15	3	0	0	0	0	0	3	0	0	0	0	3	0
16	4	1	0	0	4	4	2	0	0	0	0	0	0
17	5	0	0	0	0	1	1	0	5	4	0	0	4

Intensity (max: 100%) 100–67% 66–33% 32–1%

Key: Ant—anterior or cranial, FMFZ—frontonasal mass fusion zone, LNP—lateral nasal prominence, Md—mandibular prominence, Mxp—maxillary prominence, Post—posterior or caudal, prox—proximal.

[a] Frequency overlaid with colorimetric intensity data.

and 17 (Figs. 2D,G), there was considerably more expansion of labeled area in the stage 13 when compared to the stage 17 embryo (Figs. 2B,M; Table 1A,C). Expansion of label occurs by a combination of cell division and possible cell movement. At most, two areas with labeled cells derive from each injection site in the stage 17 embryo compared to as many as four different regions with label arising from a single injection site at

Table 2
Labelled regions of the upper beak following injections of CM-DiL into the maxillary prominence

	Analysis of dye spread in palate							Analysis of sections			
A. Global labelling of mxp	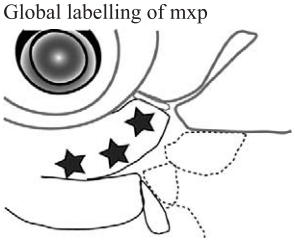										
	1	2	3	4	5	6	7		p	mxb	j
Total N (/21)	20	20	20	20	21	12	15	N = 7	5	6	7
%	95.2	95.2	95	95.2	100	57	71				
B. Labelling of cranial mxp	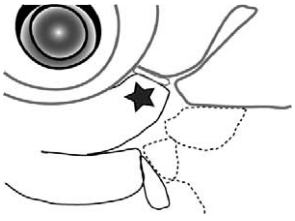										
	1	2	3	4	5	6	7		p	mxb	j
Total N (/18)	18	18	13	7	5	1	0	N = 5	4	5	1
%	100	100	72	39	28	6	0				
C. Labelling of caudal mxp	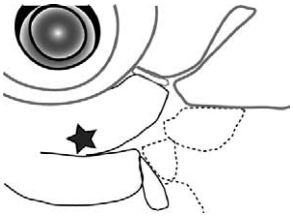										
	1	2	3	4	5	6	7		p	mxb	j
Total (/11)	0	4	0	11	11	5	8	N = 4	3	1	2/2
%	0	36	0	100	100	45	73				

Key: j—jugal, mxb—maxillary bone, mxp—maxillary prominence, np—nasal pit, p—palatine bone, pmx—premaxilla.

stage 13. This may reflect the rapid growth of the embryo during these stages.

Injection sites in the post-optic region make the major contribution to the maxillary prominence

As soon as the pharyngeal arches form at stage 13, there are already cells that contribute to the maxillary prominence with origins outside the confines of the mandibular arch. Injections close to the maxillo-mandibular cleft demonstrated that cells (site 1, Fig. 2B; Table 1A) populated the caudal maxillary prominence, lateral mandibular prominence, and the area proximal to the maxillary prominence. In contrast, cells labeled in the post-optic region contributed to the maxillary prominence (sites 13 and 16, Fig. 2C; Table 1A). A similar pattern was repeated at stages 15 and 17 although it was possible to resolve more clearly the contributions of post-optic region at later stages. There were at least five locations in the post-optic region that made contributions to the maxillary prominence (sites 1, 12, 13, 15, 16, Figs. 2E,F,H,I,N,O; Table 1B,C; and data not shown). By stage 17, however, site 1 gave only a minor contribution to the caudal maxillary prominence and most labeled cells remained proximal to the prominence (Fig. 2M).

In order to determine how much cell mixing occurred between cells labeled site 1, the maxillo-mandibular cleft and site 13 beneath the eye, we performed dual DiI and DiO injections at stage 15 (Fig. 2K). In these specimens, the two groups of cells were widely separated by stage 24 (n = 8/8), indicating that cells remain in approximately the same locations as their original labeling site. The data from the two-color injections in addition to that from single injections showed there were different origins for the cranial and caudal maxillary prominence (cranial—sites 12, 13, 15, and 16; caudal—sites 1 and 16).

The zones of fusion between upper facial prominences were mapped to precise locations in the pharyngeal arch-stage embryo

In order to map the origins of some of the other facial prominences, injections were carried out medial to the eye and just inferior to the eye. No injections were made medial to the nasal pit since we had previously shown this region remains in the frontonasal mass (Lee et al., 2001). The lateral nasal prominence originated as predicted, from sites 14 and 17 (Figs. 3A–D). We were also able to label specifically the future site of the nasolacrimal groove (sites 14 and 17), which defines the most cranial aspect of the maxillary prominence (Figs. 3A–D; Table 1B). Merging of the lateral nasal and maxillary prominence eventually smoothes out this groove and the nasolacrimal duct forms

Table 3
Analysis of bones from stage 24 maxillary prominence grafts

(A) Number of bones developed per maxillary prominence graft

	1	2	3	>3
Cranial (N = 10)	2	6	2	0
Caudal (N = 18)	9	9	0	0
Whole (N = 19)	0	12	4	3

(B) Types of bones formed in each maxillary prominence graft

	Whole palatine[a]	Maxillary process of palatine[b]	Posterior process of palatine[c]	Jugal[d]	Maxillary[e]	Jugal + maxillary bone fused[f]	Grafts with unidentifiable bones[g]
Cranial (N = 10)	0	4	0	4	5	3	1
Caudal (N = 18)	0	10	1	7	1	1	7
Whole (N = 19)	4	2	6	12	12	4	3

[a] A bone with one elongated process and opposite end is broad. Trabeculae are orientated along long axis of bone.
[b] A thick bone with elongated shape, ends do not have any secondary processes. Trabeculae are orientated along long axis of bone.
[c] Broad bone, diamond in shape with no process any longer than the rest. Trabeculae are orientated along long axis of bone.
[d] Trabeculae randomly orientated, usually elongated, narrow in diameter with tapering ends.
[e] Trabeculae randomly orientated, roughly diamond shaped with several short processes, small.
[f] Characteristics of maxillary bone with one very long process.
[g] Bones that are spherical, small with no identifiable processes.

from the deeper tissue. Our fate map places the origins of this groove mid-way between the eye and the nasal placode. We were also able to specifically target the future site of fusion zone between the frontonasal mass and maxillary prominences. The maxillary contribution to this fusion zone originated inferior to the eye primordium (site 12,15) whereas the frontonasal contribution is partly from sites 14 and 17 (Figs. 3H–J). These are the first fate mapping data for regions affected in human cleft lip with or without cleft palate.

Midline condensations are derived from lateral progenitor cells

The only exceptions to the rule that cells expanded and remained in approximately the same relative position after 48 h of growth were sites 12 and 15, directly inferior to the eye. These injection points gave rise to labeled cells close to the midline of the stomodeum as well as cells within the cranial maxillary prominence (Figs. 3E–G). These data suggest that the midline condensations, which are composed of the trabeculae cranii and intertrabecula (Bellairs, 1958), are derived initially from more lateral locations close to the eye primordia. The trabecular condensations merge and give rise to the interorbital and nasal septum. Most other injection sites did not spread toward the midline; however, it is likely that formation of the tissue buds erected a physical barrier to expansion.

Gene expression patterns suggests that different molecular codes exist in the cranial and caudal maxillary prominence

We examined expression of several genes at slightly different stages of development starting at stage 14 in order to see whether there were expression patterns that correlated with the different origins for the caudal and cranial maxillary prominence. There were three patterns observed. The first was exemplified by expression in both the maxillary post-optic region and the mandibular arch present from the onset of pharyngeal arch morphogenesis and prior to maxillary bud formation at stage 18. *Tbx2* (T-box containing transcription factor) transcripts were expressed in all regions of the forming face including lateral nasal and frontonasal mesenchyme perhaps marking a mesenchymal population with common characteristics and common origins (Fig. 4A). *Fgf8* was expressed in first pharyngeal arch epithelium only (Figs. 4B,C) and then later in the maxillo-mandibular cleft epithelium (data not shown, see also Shigetani et al., 2000).

The second pattern was represented by two other transcription factors, *Barx1* and *Msx1*. These genes were expressed in the first pharyngeal arch (Figs. 4D,E,G,H) but expression only appeared in the maxillary prominence once it had formed (Figs. 4F,I; see also data from Shigetani et al., 2000). Expression of *Barx1* in the stage 20–28 maxillary prominence was strong caudally but rapidly decreased towards the cranial (Fig. 4I; Barlow et al., 1999). Epithelial *Fgf8* signal overlies the caudal expression of *Barx1* (data not shown). We and others found that *Msx1* had almost a complementary pattern to *Barx1* with high expression cranially and low expression caudally (Fig. 4F; Lee et al., 2001; Shigetani et al., 2000). Due to the fact that these restricted expression patterns appear relatively late in relation to maxillary prominence formation, it is possible that these may be set up by preexisting differences in the cranial and caudal mesenchyme.

The third pattern we observed was restricted expression in the early stage 14 post-optic region that marked

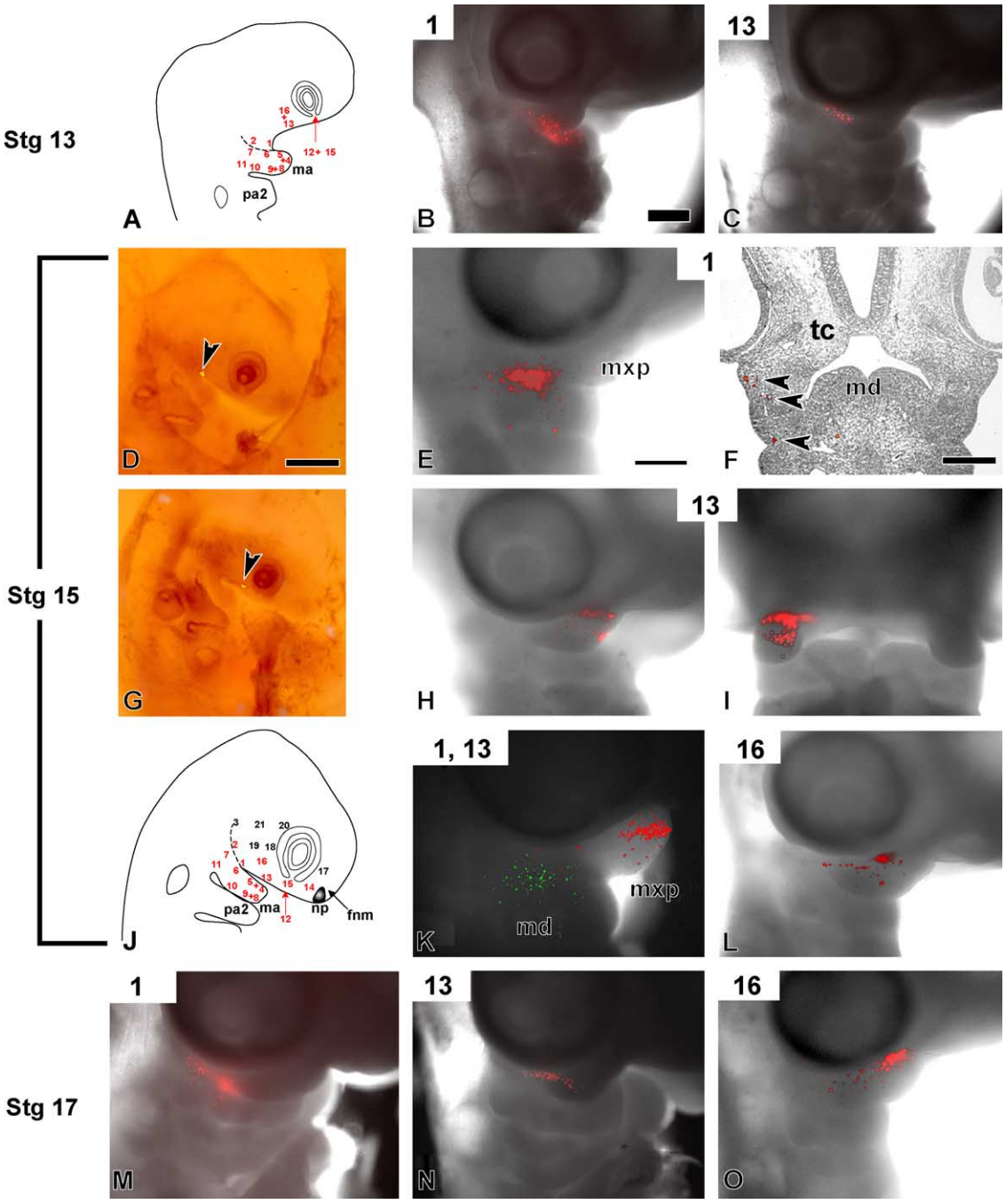

Fig. 2. Spread of DiI from injection into the maxillo-mandibular cleft and post-optic regions. Fluorescent images have been superimposed on bright field views in all panels. Injection site numbers for each embryo are indicated in white boxes. (A) Diagram for injection sites. (B) Dye has spread into mainly the cranial side of the mandibular prominence and caudal maxillary prominence. (C) Dye is mainly in the caudal maxillary prominence. (D) Neutral red stained embryo showing injection site 1. Note the very localized point of dye. (E, F) Same embryo showing surface and sectioned view with labeled cells in the lateral mandibular prominence and caudal maxillary prominence. (G) Injection site 13. (H, I) Same embryo showing very little medial spread of the dye. Cranial maxillary prominence is labeled. (J) Positions of dual injection of DiI (red) and DiO (green). (K) Confocal slices from approximately 200 μm in depth merged into one file. There is no overlap of dye, showing very little cell mixing taking place between these two injection points. (L) Injection into the post-optic region exclusively targets the cranial maxillary prominence. (M, N, O) Similar patterns in stage 17 embryos; however, extent of dye spread was not as great at with younger stages. Key: fnm—frontonasal mass, ma—mandibular arch, md—mandibular prominence, mxp—maxillary prominence, pa2—second pharyngeal arch, tc—site of future cell condensation for trabeculae cranii. Scale bars = 0.5 mm for all photographs.

the same area that contributes to the cranial maxillary prominence, lateral nasal prominence and globular process. *Bmp2* and *Bmp4* transcripts were localized mainly in the post-optic region with some additional expression noted in the distal mandibular arch (Figs. 5A–C). *Rarβ* transcripts had been described by us previously (Rowe et

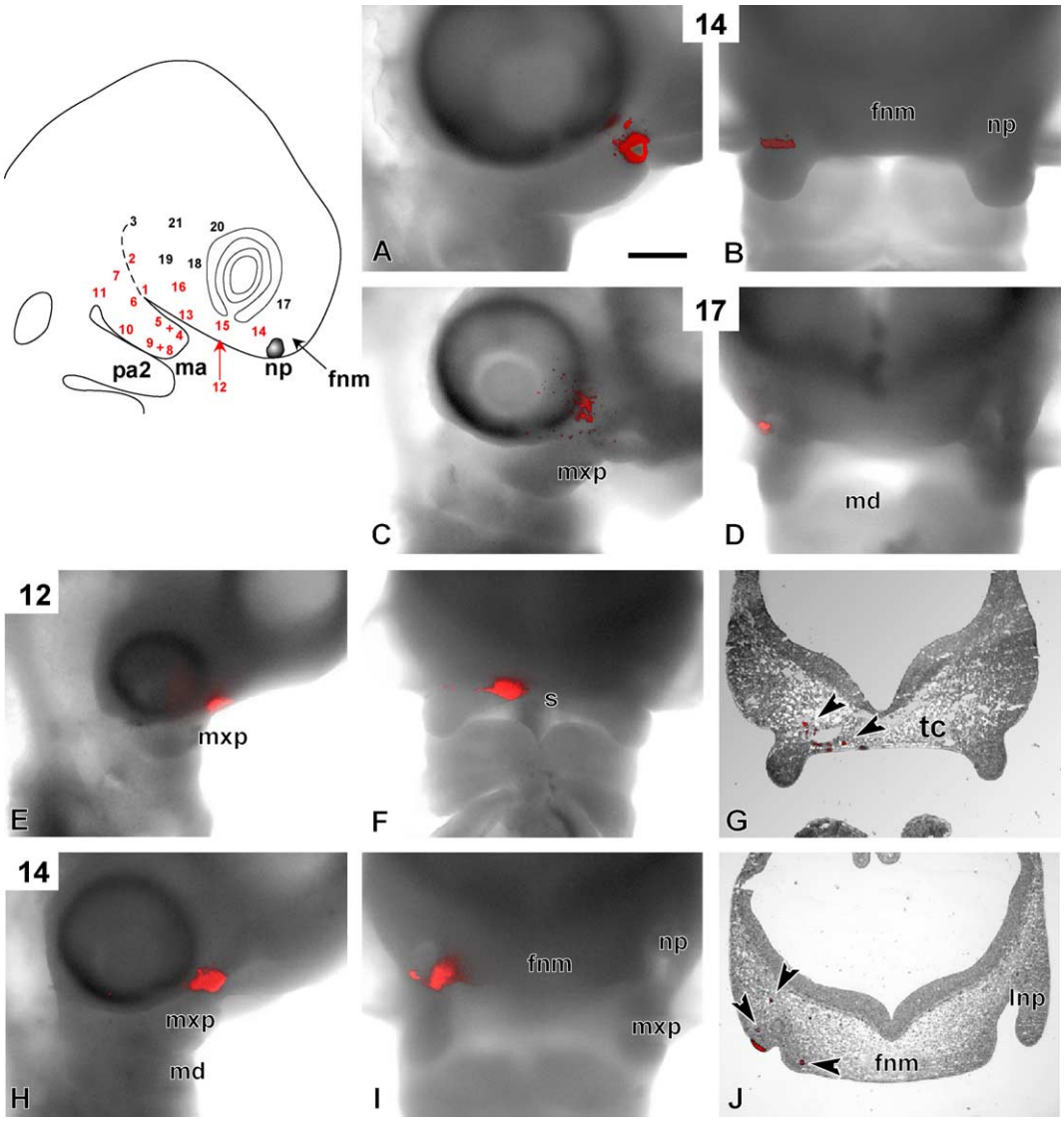

Fig. 3. Dye spread into the stomodeum and frontonasal mass. Fluorescent images have been merged with bright-field images. (A, B) Labeled cells are found in the cranial maxillary prominence close to the nasolacrimal groove. (C, D) Cells in the nasolacrimal groove are labeled. (E–G) Same embryo in each picture showing cells have moved medially into the stomodeum. Section shows labeled cells in the future site of the trabeculae cranii. (H–J) Views of the same embryo showing bright label in the globular process of the frontonasal mass. Key: fnm—frontonasal mass, lnp—lateral nasal prominence, ma—mandibular arch, md—mandibular prominence, mxp—maxillary prominence, np—nasal pit, pa2—second pharyngeal arch, s—stomodem, tc—site of future cell condensation for trabeculae cranii. Scale bars = 0.5 mm for all photographs.

al., 1991) but not in whole embryos. It is clear that *Rarβ* is expressed more than 24 h prior to the formation of the maxillary bud (Figs. 5D–F). Once the maxillary prominences forms, expression of *Bmp2*, *Bmp4*, and *Rarβ* are restricted to the cranial mesenchyme and epithelium (Fig. 5G; Ashique et al., 2002a; Francis-West et al., 1994; Rowe et al., 1992). There appears to be a regionally specific code of gene expression in the cranial and caudal halves of the maxillary prominence that suggests different origins and different fates (in terms of pattern) for these regions. Some genes appear to carry with them information about which cells are cranial and other genes become patterned once the prominence has formed.

Determination of maxillary prominence derivatives

Until the present study, there had never been any direct fate mapping of the maxillary prominence. We had derived some fate information through grafting of facial prominences to ectopic locations in host embryos; however, we had not previously stained these grafts for ossification in whole mount (Lee et al., 2001; Richman and Tickle, 1989). Furthermore, sections of maxillary grafts could not be used to identify specific bones (Richman and Tickle, 1989). In order to determine the skeletal elements derived from the maxillary prominence, we carried out two different experiments, both of which began at stage 24, the stage at which we ended our first series of observations. The first experi-

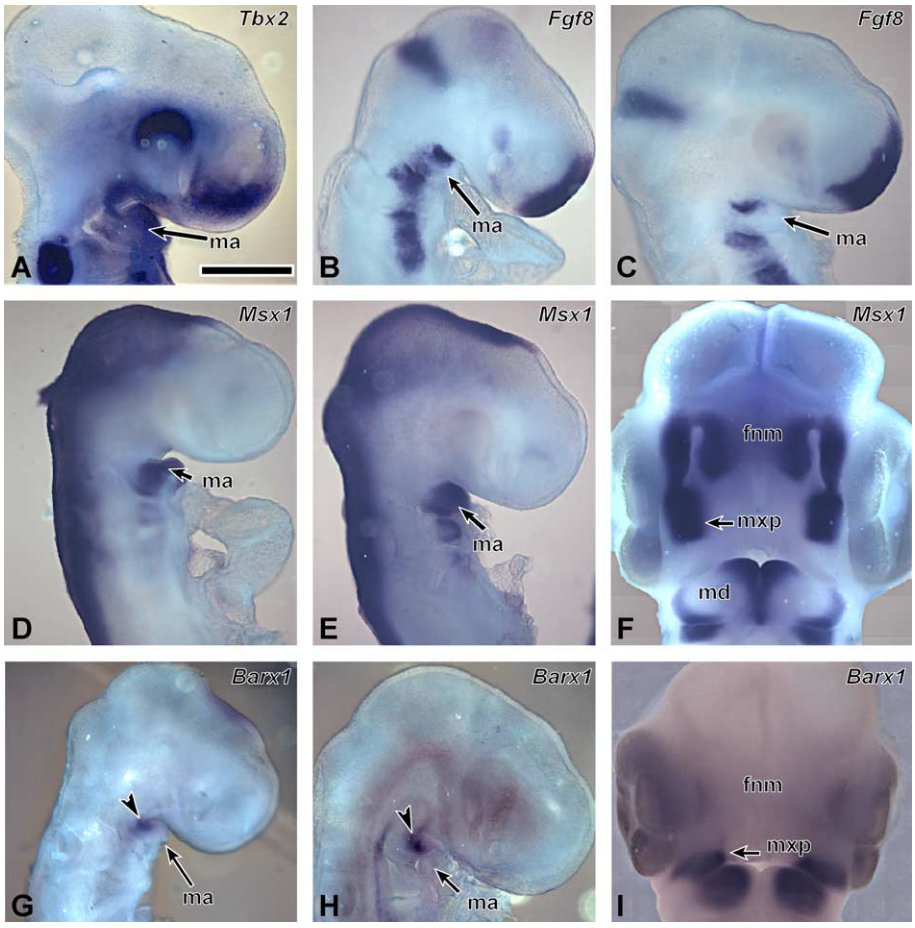

Fig. 4. Expression of homeobox transcription factors and *Fgf8* in staged embryos. (A) *Tbx2* expression is simultaneously expressed in the first pharyngeal arch and cranial, post-optic region at stage 15. (B) Stage 14.5 embryo with expression in the cranial side of the mandibular arch and in the lateral surface ectoderm. (C) Stage 15 embryo with decreased expression in the lateral surface of the mandibular arch. Down-regulation occurs between 23 and 27 body somites. (D, E) Stages 14 and 15 embryos with localized expression in the mandibular arch only but not in the post-optic region. (F) Stage 24 embryo showing strong induction of signal and a clear boundary between expressing and nonexpressing tissue midway through the maxillary prominence. (G, H) Stages 14 and16 embryos with signal only present in the proximal mandibular arch. (I) Later, at stage 24, expression is induced with a sharp boundary within the maxillary prominence. Note expression is complementary to F in both the maxillary prominences and mandibular prominences. Key: fnm—frontonasal mass, ma—mandibular arch, md—mandibular prominence, mxp—maxillary prominence. Scale bar = 0.5 mm.

ment was focal dye labeling with CM-DiI of cranial, caudal or several places in order to label most of the maxillary prominence. The second experiment was to graft either whole or bisected maxillary prominences to host limb buds in order to allow autonomous development to occur outside of the face. Both experiments were terminated at stages where the maxillary, jugal, palatine, and quadratojugal had ossified in the intact embryo.

Macroscopic inspection of embryos originally injected in cranial, caudal, and central locations (Figs. 6D,G), the majority of the palate could be labeled (Figs. 6E,H). The label extended from the medial edge of the palatal shelf (normally not fused in the chicken) laterally to encompass the tomium (edge of the beak, Figs. 6E,H). The most distal extent of label ended short of the tip of the beak suggesting that the prenasal cartilage and premaxilla were not derived from the maxillary prominence (Table 2A). Sections of a subset of embryos (Table 2A) allowed us to determine precisely that the dye had labeled cells in the maxillary, jugal, palatine bones (Table 2A; Figs. 6F,I) as well as the surrounding connective tissue. It was also clear that labeled cells did not contribute to the premaxillary bone or prenasal cartilage (data not shown). Interestingly, the connective tissue between the premaxilla and maxillary bone was labeled, which is where the zone of fusion occurred at earlier stages of primary palate development (data not shown). In sections through the quadratojugal, only a few labeled cells were seen, reflecting the localization of injections to the mesenchyme at the distal edge of the maxillary prominence (Figs. 6E,H,K,N).

Grafts of whole maxillary prominences were also informative. In general, two to three bones formed in each graft (Table 3A) and for the most part these could be identified as the palatine, jugal, and maxillary bones (Figs. 7C–L; Table 3B). A proportion of the grafts formed more than three bones (n = 3/19), which may indicate that a portion of the quadratojugal had formed; however, it was

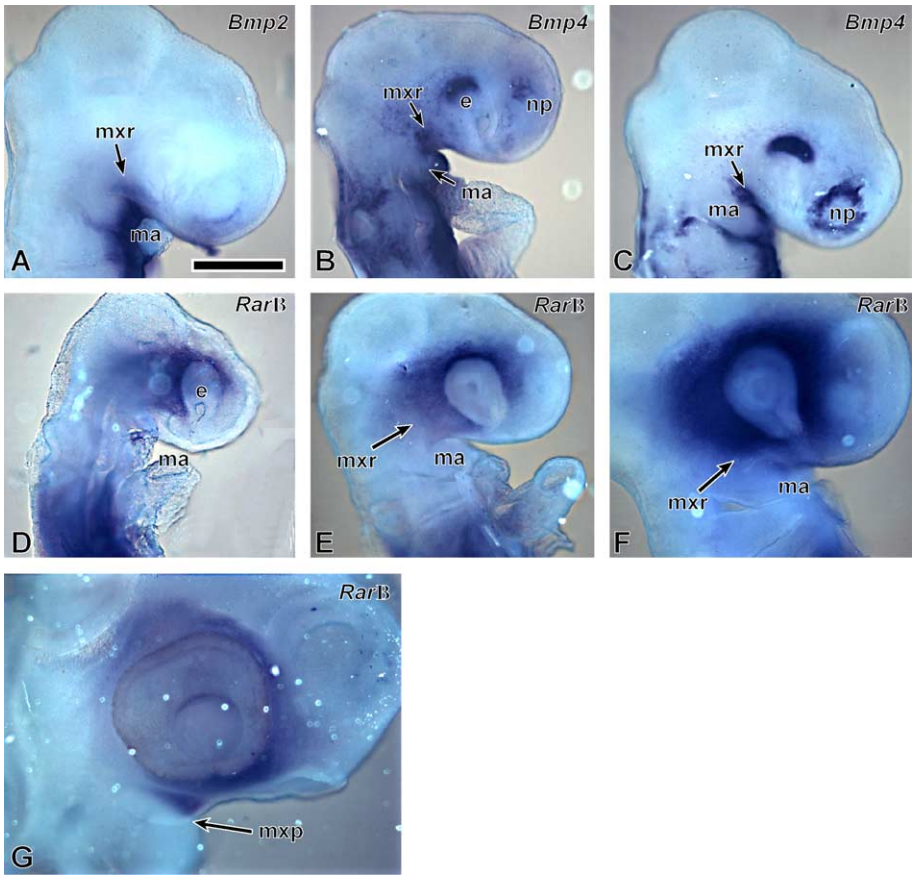

Fig. 5. Expression of genes in the BMP and RA pathways, *RARβ*, *Bmp2*, and *Bmp4*. (A) Expression in the post-optic maxillary region and medial mandibular arch at stage 15. (B, C) Expression at stages 14 and 15 in the epithelium covering the maxillary region and in the nasal placode. (D, E, F) Stages 14, 14.5, and 15 embryos showing signal both cranial and caudal to the eye, coinciding with injection sites 16 and 13. No detectable signal in the mandibular arch. (G) At stage 24 and as soon as the maxillary prominence forms (stage 18), there is a sharp boundary of expression in the cranial prominence. Key: e—eye, ma—mandibular arch, mxr—maxillary region, mxp—maxillary prominence, np—nasal placode. Scale bar = 0.5 mm.

not possible to definitively identify this bone (Fig. 7I). Thus, in combination with the dye labeling data (Table 2A), we determined that the maxillary, jugal, and palatine bone were derivatives of the maxillary prominence.

Our first set of fate maps and gene expression studies had suggested that there were different cell populations contributing to the cranial and caudal maxillary prominences. We therefore asked whether there was a difference in the fate of these two regions. Dye injected at the cranial edge of the prominence (Fig. 6J) contributed to distal regions of the palate but did not extend to the distal tip of the beak (Table 2B; Fig. 6K). Microscopic analysis showed that the maxillary and palatine bones were labeled while the jugal bone was less often labeled (Table 2B; Fig 6L). In addition to bones being labeled, there was labeling of the connective tissue between the maxillary and palatine bones (Fig. 6L). Grafts of the cranial half of the maxillary prominence gave rise to fewer bones than the whole maxillary prominence consistent with the idea that we were omitting some skeletal elements. In the majority of cases, grafts contained maxillary and jugal bones (Table 3, data not shown). If the palatine bone was present, only the maxillary process was included (n = 4/10).

Caudal injections (Fig. 6M) labeled proximal parts of the palate from the midline extending out to the tomium (Fig. 6N). Sections revealed dye-labeled cells in the body of the palatine bone and the jugal (Fig. 6O) and only infrequently the maxillary bone (Table 2C). Grafts of the caudal half included either one or two bones (n = 9/18 for each), less than grafts of whole prominences again, suggesting that we had omitted some of the maxillary derived skeletal elements. The majority of grafts formed palatine bone (n = 11/18) while the maxillary bone was formed only infrequently (n = 2/18). Thus, although bisected the maxillary prominence arbitrarily through the center, we were able to show a difference in the derivatives from cranial and caudal halves. The combination of dye and graft data indicated that more caudal derived cells were mainly contributing to proximal upper beak elements whereas cranial-derived cells contributed the distal elements, ending at the premaxilla.

Discussion

The fate maps we have constructed for the first visceral arch began shortly after the arch forms and continued until

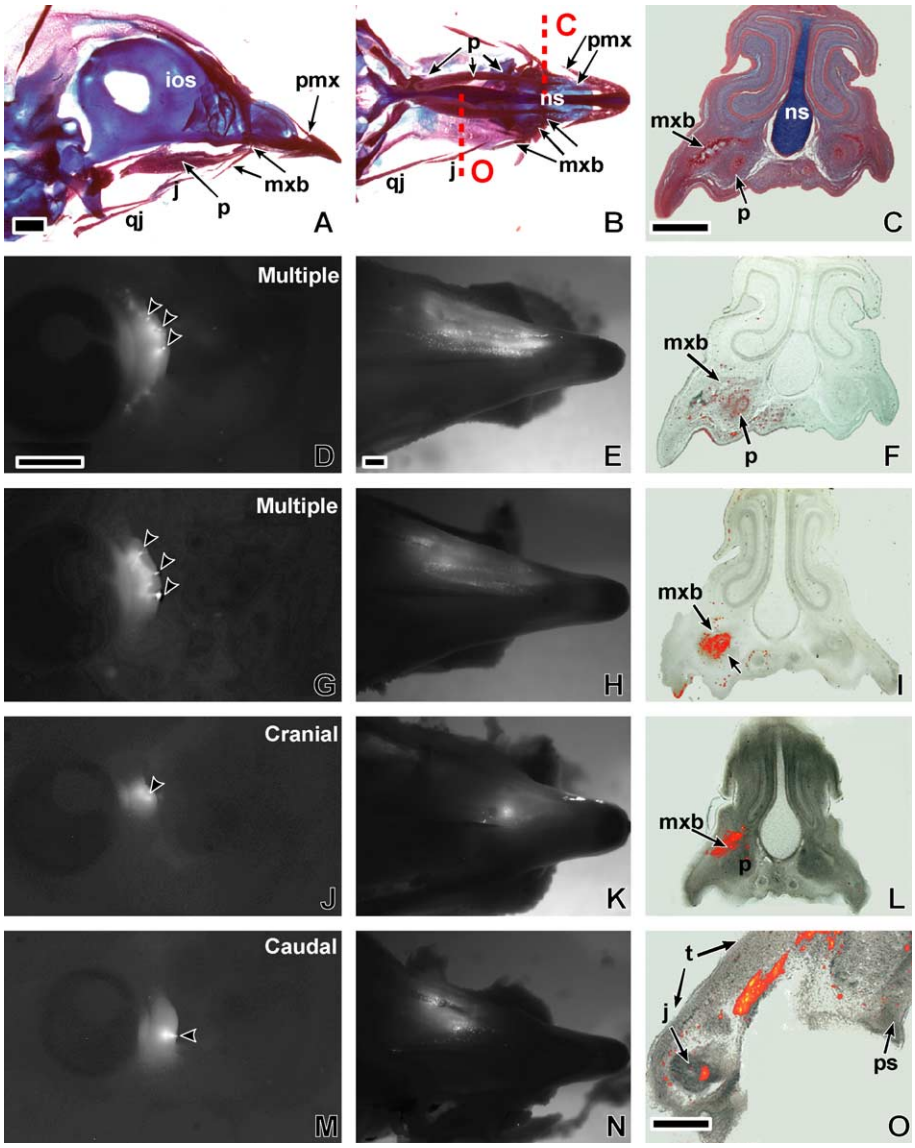

Fig. 6. Contributions of the maxillary prominence to the upper beak. (A, B) Skeletal preparations of stage 34 skulls. Approximate planes of section for panels C, F, I, L are indicated by dashed line marked "C" and plane of section for panel O is indicated by dashed line marked "O". (C) Example of Picosirius Red/Alcian Blue stained section adjacent to the one in panel G. D, G, J, M were taken with Rhodamine fluorescence illumination in ovo. E, H, K, N are fixed embryos photographed from the palatal view with the mandible removed. F, I, L, O represent merged bright-field and fluorescence images. Each row, beginning with panel D, represents longitudinal examination of a single specimen first at 3–6 h post-injection, second at fixation and then after sectioning the tissue. (E–G) Dye was injected in several locations to label the majority of the maxillary prominence. The outcome was the labeling of a large portion of the palate, but not including the tip of the beak (E). Sections showed labeled cells in the maxillary bone and palatine bone as well as adjacent connective tissue (compare F to panel C). (G–I) Similar outcome for a specimen labeled in multiple locations in the maxillary prominence. (J–L) Injection targeted to the cranial aspect of the maxillary prominence labels a smaller part of the palate and mainly the maxillary bone. (M–O) Label in the caudal part of the maxillary prominence results in a complementary pattern to that seen in panel L. Sections demonstrate label in the jugal bone and extending to the tomium. Key: ios—interorbital septum, j—jugal, qj—quadratojugal, mxb—maxillary bone, ns—nasal septum, p—palatine bone, pmx—premaxilla, ps—palatal shelf, t—tomium. Scale bars: bar in A applies to A and B and is 1 mm; bar in C is 500 μm and applies to F, I, L; bar in D is 1 mm and applies to G, J, M; bar in E is 1 mm and applies to H, K, N; bar in O is 250 μm.

defined facial buds were present around the stomodeum. Cells labeled in the first pharyngeal arch remained within the mandibular prominence except for those located at the maxillo-mandibular cleft. These cells spread out cranially and caudally and contributed to the caudal edge of the maxillary prominence as well as the mandibular prominence (Fig. 8A). However, the majority of the maxillary prominence was derived from the "maxillary condensation" located between the eye and the maxillo-mandibular cleft rather than the first pharyngeal arch (Fig. 8A). In keeping with distinct fates for the first pharyngeal arch and maxillary condensation, we also found that there was a molecular code of gene expression that differed in these two regions. In addition, as the maxillary bud grew out in

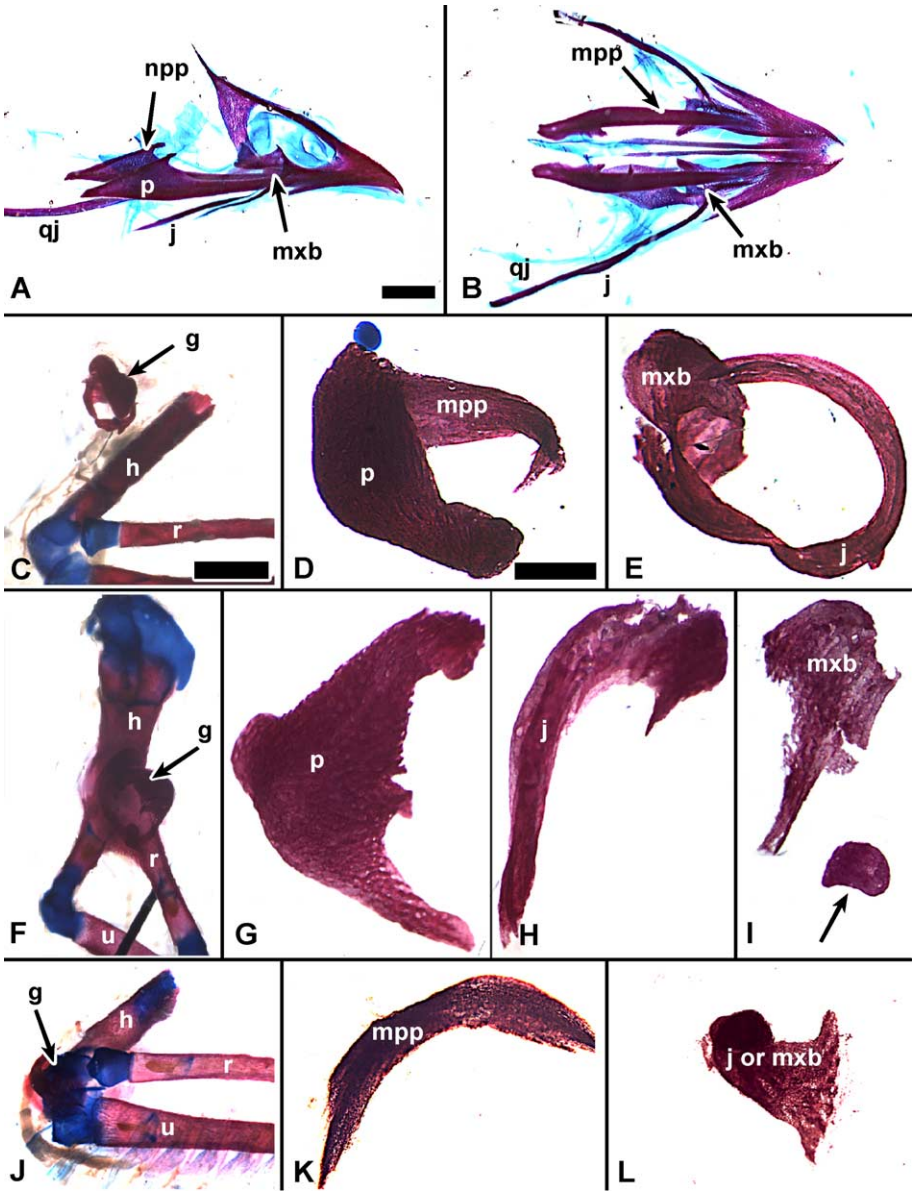

Fig. 7. Development of bones within grafts to the limb bud of stage 24 maxillary prominences. (A) Dissected stage 38 upper beak skeleton, sagittal view. Body of the palatine bone is thicker and lined with organized trabeculae. (B) Palatal view of upper beak skeleton showing the relationship of the maxillary process of the palatine bone to the maxillary bone. (C) Graft of whole maxillary prominence formed separate skeletal elements adjacent to the humerus. (D) One of two dissected bones from graft in C. The bone is thick with well-organized trabeculae and has one elongated process resembling the body of the palatine bone with the maxillary process. (E) Second dissected bone from graft in C. There is a long narrow bone resembling the jugal fused to a broad flat bone with several processes resembling the maxillary bone. (F) Graft of whole maxillary prominence in close apposition to the humerus. (G) First of four dissected elements from the graft has thick trabeculae and resembles the body of the palatine bone with short nasal and maxillary processes. (H) Elongated bone with less organized trabecular structure, resembling the jugal. (I) Smaller bone with at least one long process similar to the jugal process of the maxillary bone. And additional bone nodule has formed with no distinct processes (arrow). (J) Graft of a posterior segment of the maxillary prominence, adjacent to elbow joint. A total of two bones were contained in the graft, (K) one similar to the maxillary process of the palatine, as judged by bone quality and (L) a smaller bone that could be either the maxillary or jugal bone. Key: g—graft, h—humerus of host limb, j—jugal, qj—quadratojugal, mpp—maxillary process of the palatine bone, mxb—maxillary bone, npp—nasal process of the palatine, p—body of the palatine bone, r—radius, u—ulna. Scale bars: bar in A, B = 2 mm; bar in C applies to F, J and is 1 mm; bar in D applies to E, G–I, K, L and is 500 μm.

response to local signals, gene expression patterns were carried forward (Fig. 8B). Our second-stage fate maps showed that mesenchymal cells from cranial maxillary prominence gives rise to the distal maxillary bone and maxillary process of the palatine bone whereas the proximal body of the palatine bone and jugal bone derive from caudal mesenchyme. We link our data on the pharyngeal arch stages of morphogenesis to full skeletal patterning to show for the first time the embryonic origins of the upper jaw bones.

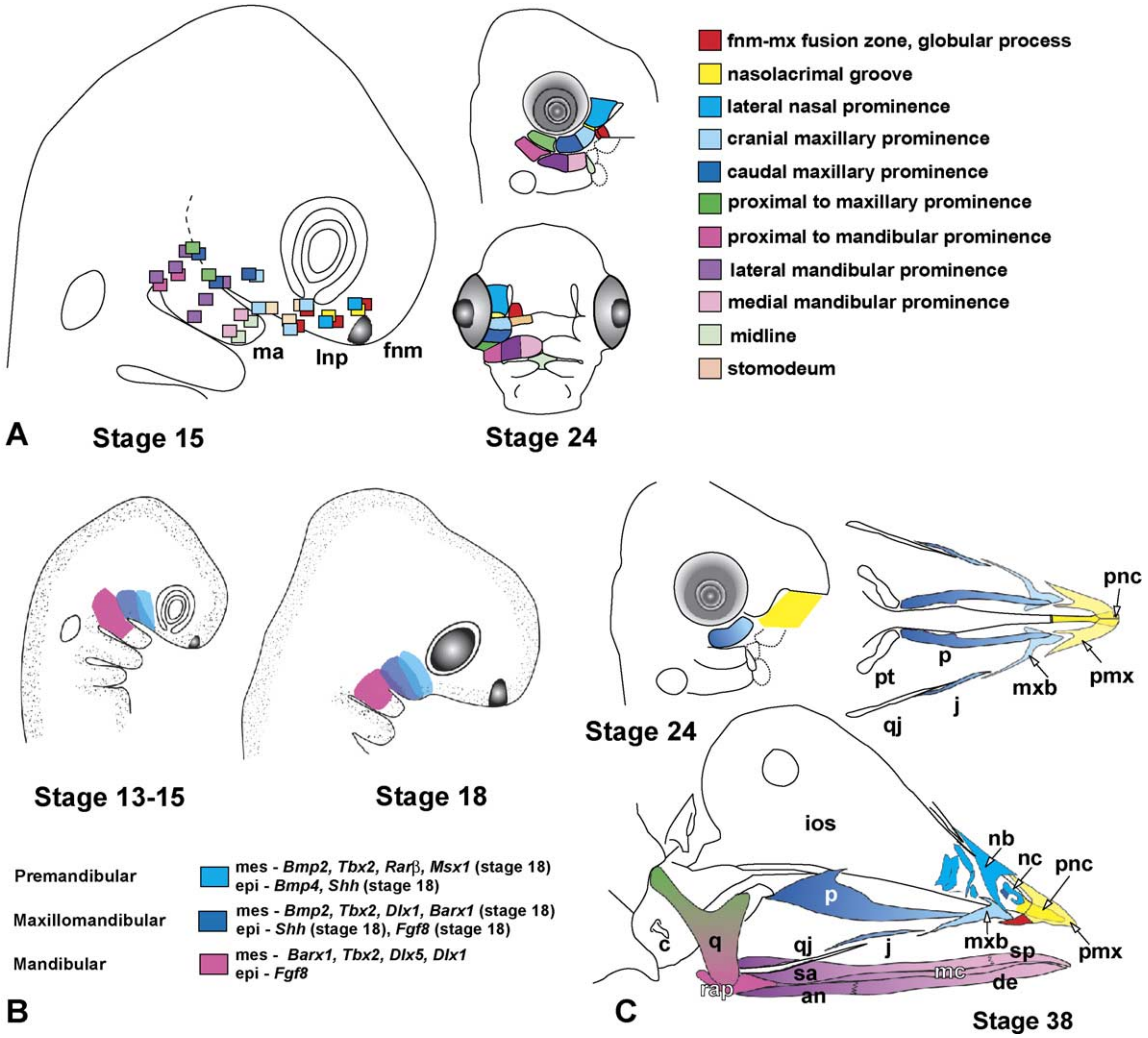

Fig. 8. Summary of the origins and fate of the maxillary prominence. (A) The fate of labeled cells projected onto a stage 15 embryo according to analysis of subdivisions of the stage 24 facial prominences. Movement of labeled cells is observed from the lateral to the medial side of the nasal pit ultimately, contributing to the globular process of the frontonasal mass and zone of fusion. No significant difference was observed in contributions from injections done along the cranial or caudal side of the mandibular arch. All sites contribute to the mandibular prominence. The majority of the sites labeled in the post optic region and beneath the eye contributed to the maxillary prominence. (B) Stages 13–15, the drawing illustrates the transition from pharyngeal arch stages until the formation of a distinct maxillary bud. Cells in first pharyngeal arch remain largely in this region. Cells from the premandibular and maxillo-mandibular region give rise to the maxillary prominence. The division of the post-optic region into the premandibular and maxillo-mandibular based on dye labeling and gene expression results as well as the data from others (Shigetani et al., 2000). Note that all expression domains for a gene are not illustrated here. Rather, the expression of genes in the area under investigation is listed. Stage 18, all three regions make a contribution to the maxillary prominence, although the mandibular arch contribution is relatively less than the other two. This model contrasts data from Shigetani et al. (2000), which suggests the premandibular region does not contribute to the maxillary prominence. (C) Stage 24 embryo showing cranial to caudal axis in the maxillary prominence by light to dark blue, respectively. Yellow indicates the frontonasal mass. Stage 38 colorized skeleton from palatal and side views, indicating regions of facial prominences that have been shown through experiments to contribute to certain skeletal elements. Data for the maxillary, palatine, and jugal are from this paper and from Barlow and Francis-West (1997); data for the mandible is taken from Richman and Tickle (1989); data for the quadrate is taken from Wilson and Tucker (2004); data for the nasal bone and chonchae is from Song and Richman (unpublished data) and from MacDonald et al. (2004). Areas left white including the quadratojugal and pterygoid have no direct experimental evidence of their origins. The gradient of color is to indicate that there are no sharp boundaries in the maxillary prominence that reflect lineage-specific compartments. Key: an—angular bone, c—columella, de—dentary, epi—epithelium, fnm—frontonasal mass, lnp—lateral nasal prominence, ios—interorbital septum, j—jugal, q—quadrate, qj—quadratojugal, ma—mandibular arch, mc—Meckels' cartilage, mes—mesenchyme, mx—maxillary prominence, mxb—maxillary bone, nb—nasal bone, nc—nasal conchae, p—palatine bone, pmx—premaxilla, pnc—prenasal cartilage, pt—pterygoid, rap—retroarticular process, sa—superangular, sp—splenary.

How early does the maxillary region become distinct from the mandibular?

Neural crest fate mapping using quail chicken chimeras provides the evidence that the distal upper and lower beak skeletal elements share common origins in the mesencephalon (Kontges and Lumsden, 1996). However, unlike in the hindbrain, there are no distinct streams of cells coming out of the neural tube cranial to rhombomere 3. Nonetheless, there is very little cell mixing cells originating in the

mesencephalon–diencephalon isthmus with those from the mesencephalic–rhombencephalic (Shigetani et al., 2000). Once pharyngeal arches begin to form (stage 13), *Bmp4* and *Fgf8* can be detected in the presumptive first pharyngeal arch ectoderm at stage 13, but not in the ectoderm covering the post-optic, presumptive maxillary condensation (Shigetani et al., 2000). Our results at stage 14 show that distinct molecular patterns are being developed in the ectoderm of the maxillary region with *Bmp4* being expressed earlier than *Fgf8* (Fig. 8B). In the mesenchyme, there are also early differences between the maxillary condensation and first pharyngeal arch with *Rarβ* being uniquely expressed in the post-optic region, whereas *Msx1* and *Barx1* are initially only expressed in the first pharyngeal arch (see also data from Shigetani et al., 2000). The relative lack of cell mixing that occurred in the dye labeling of the maxillary condensation and first visceral arch, together with these gene expression patterns suggests that unique maxillary and mandibular identity is already established by the time the first pharyngeal arch forms.

There are some functional data to show that the two epithelial signals, FGFs and BMPs, can alter patterning of the first pharyngeal arch and maxillary region. Ectopic increase in FGF8 and BMP4 in the maxillary region affects the expression of mesenchymal genes and patterning of the trigeminal nerve (Shigetani et al., 2000). The identity of the jaw skeleton appears not to be affected although it is hard to be certain since the effect on bones was not examined in these experiments (Shigetani et al., 2000). Now that we have shown distinctiveness in the origin of cells that contribute to the maxilla and mandible, it is reasonable to expect that differences in local signals are responsible for specifying upper versus lower jaw identity.

Origins of the trabeculae cranii and interorbital septum are not in the midline of the embryonic face

The injection of dye beneath the eye surprisingly resulted in label of the center of the stomodeal roof. A day later (stage 26, E5) the midline mesenchyme of the stomodeum condenses beneath the brain to form the laterally positioned trabeculae cranii and intertrabeculae that eventually merge with the interorbital septum (Bellairs, 1958; Cerny et al., in press; de Beer, 1931). The interorbital septum and nasal septum develop as one continuous structure, extending in a cranial direction (de Beer, 1937). The trabeculae cranii and the derived interorbital septum are positioned cranial to the maxillary bones in amniotes. Little experimental work has been carried out on the origins of these midline cartilages (Bellairs, 1958); however, excision of the frontonasal mass at later stages did not affect development of the interorbital and nasal septum (McCann et al., 1991) demonstrating that the septal cartilages, although neural crest derived (Couly et al., 1993), are not derived from the frontonasal mass. The data from the accompanying paper by Cerny et al. (in press) demonstrate that in chicken and axolotl cells derived from area inferior to the eye contribute to the cartilage condensations of the trabeculai cranii. These fate maps in combination with our data from stage 26 embryos show that the origins of the interorbital septum and nasal septum (both of which are part of the neurocranium) are in fact quite lateral. We know from our previous work that Noggin and RA signals are important for specifying the interorbital septum (Lee et al., 2001). It is likely that in these experiments, the reagents were able to diffuse from the bead and thus affect the mesenchyme beneath the eye, fated to make the midline neurocranial cartilages.

Proximo-distal patterning in the beak is established prior to maxillary prominence formation

We are now able to relate proximo-distal patterning of the upper beak to the origins of the maxillary prominence. We can discern differences in the cranial versus caudal cells within the maxillary condensation in terms of their positions in the upper beak. Those that are cranial give rise to the maxillary bone, and the maxillary process of the palatine bone, whereas the more caudal cells contribute to more proximal elements such as the jugal and body of the palatine bone. It is likely that the group of cells from the maxillo-mandibular cleft contribute to the most proximal element of the upper beak, the quadratojugal. Therefore, the cranial–caudal axis of the maxillary prominence becomes the proximo-distal axis of the beak once fusion has taken place and the beak tips outwards from the head.

It is interesting that a previous investigation defined two separate regions between the maxillo-mandibular cleft and the eye, the premandibular region that is directly adjacent to the eye, and a more caudal, maxillo-mandibular region adjacent to the maxillo-mandibular cleft (Fig. 8B; Shigetani et al., 2000). These authors found that different regions of the mesencephalic neural crest contributed to the two post-optic areas. We agree that there may be two subregions between the eye and maxillo-mandibular cleft; however, we have come to different conclusions about the fate of these regions. Shigetani et al. (2000, 2002) have stated that the premandibular region does not contribute to the maxillary prominence. Our results show that cells from the entire post-optic region contribute to the maxillary prominence and that the premandibular segment contributes to the maxillary and palatine bone whereas the maxillo-mandibular segment forms the palatine and jugal bones.

The zones of fusion and merging in the primary palate

In addition to patterning the skeleton and associated tissues, a molecular code may help to give cells from the cranial maxillary prominence different properties such as the

propensity to proliferate or undergo apoptosis. The medial side of cranial maxillary prominence makes contact with the frontonasal mass as part of the fusion of the primary palate (Ashique et al., 2002a). The fusion process requires directed outgrowth, contact of epithelia, removal of the epithelial seam through a combination of apoptosis and epithelial–mesenchymal transformation and the formation of a mesenchymal bridge. In addition, the nasolacrimal groove and later the nasolacrimal duct form between the cranial maxillary and lateral nasal prominence. Apoptosis is also prevalent in this location (McGonnell et al., 1998). Relatively less programmed cell death is observed in the caudal maxillary prominence. In addition, there is relatively higher proliferation in the cranial compared to the caudal maxillary prominence (McGonnell et al., 1998). The dye labeling experiments revealed the contributions of the frontonasal mass and maxillary prominence to the tip of the beak. We did not label the premaxilla even where the most cranial aspect of the maxillary prominence was injected with dye. We can conclude that during the normal process of fusion, mesenchymal populations from the maxillary prominence do not cross-over to the frontonasal mass. We acknowledge that different experiments are required to rule out a contribution of frontonasal mass cells to the maxillary bone.

Correlation of the maxillary bud with evolution of the upper jaw

The maxillary prominence makes such a major contribution to the upper jaw of amniotes it is interesting to consider whether more primitive gnathostomes also possesses this prominence. Surveys of craniofacial anatomy of extinct, primitive gnathostomes have been carried out by several investigators (reviewed in de Beer, 1937; Janvier, 1996); however, studies on fossils cannot assess embryonic facial development. More needs to be done with more evolutionarily ancient but extant vertebrates, at relevant embryonic stages. One such study in which scanning electron microscopy was used to describe the development of the paddlefish does not reveal a separate maxillary bud projecting from the side of the oral cavity (Bermis and Grande, 1992). Similarly, in the next most recently evolved species, amphibia, embryos do not possess a separate maxillary outgrowth (Cerny et al., 2004b; Cerny personal communication). Fish and amphibia do have maxillary bones although these are highly diverged from those seen in reptiles, birds, and mammals (Janvier, 1996). Whereas there is no debate that the bones of the upper jaw are generally homologous in different classes of animals, the question has not been addressed experimentally before in other words to test whether the embryonic origins are indeed the same. Thus, we hypothesize that a distinct facial prominence—the maxillary bud—may have been essential for evolution of the robust maxillary and palatine bones of the amniote upper jaw.

The significance of the exclusion of maxillary bones from the derivatives of the first pharyngeal arch

Many types of human congenital craniofacial abnormalities such as cleft lip with or without cleft palate are understood by relating embryonic origins to the affected structures. A similar approach is used to understand phenotypes in human genetic diseases. Many of the genetic mutations with craniofacial phenotypes such as Treacher Collins and Reiger syndrome are attributed to defects in first arch derivatives (Francis-West et al., 2003). However, the phenotype for Treacher Collins includes a reduced zygomatic bone and Reigers leads to hypoplasia of the maxillary bone. Our maps are consistent with the maxillary, zygomatic (equivalent to the jugal bone in birds) as being derived from the maxillary prominence; therefore, defects in these two syndromes should now be reinterpreted to affect a combination of first pharyngeal arch and maxillary region tissues.

Mouse genetic models in which craniofacial skeletal abnormalities are produced are similarly described according to the embryonic origins of the skeletal elements. Therefore, a series of defects described in first arch derivatives will usually include affected maxillary as well as mandibular bones (see, for example, Beverdam et al., 2002; Smith and Schneider, 1998). Our data suggests that continuing to group mandibular and maxillary defects together under the umbrella of first pharyngeal arch derivatives will lead to difficulties in the interpretation of phenotypes both in human and in mouse.

In cases where transformation of identity has occurred in the mandible such as the Hoxa2 knockout mouse and the *Dlx5/6* double knockout, interpretation is simplified with separate origins for upper and lower jaws. In the case of the *Hoxa2* knockout, the second pharyngeal arch is replaced by so-called first arch elements. However, close examination reveals that only duplicated mandibular skeletal elements form and not maxillary (Gendron-Maguire et al., 1993; Rijli et al., 1993). In the *Dlx5/6* double knockout, the mandibular bones are converted to maxillary bones and Meckel's cartilage is lost (Beverdam et al., 2002; Depew et al., 2002). Thus, again, we have only one part of the so-called first arch derivatives being duplicated. The authors interpret the *Dlx5/6* phenotype as a duplication of a part of the first visceral arch, the maxillary component. We suggest that since the maxillary component is not derived from the first pharyngeal arch, the replacement of the mandible with a maxilla is a result of the loss of first arch identity and the conversion of the first pharyngeal arch to a pair of maxillary prominences. It would indeed be interesting to know what happened to the expression of genes such as *Rarβ*, which is restricted to one section of the maxillary prominence. This would clarify whether the maxillary prominence was entirely duplicated and what in what orientation.

As part of phenotype interpretations, one is tempted to draw conclusions about evolution of jaws (discussed in depth by Smith and Schneider, 1998). The *Dlx5/6* knockout

phenotypes were suggested to be an atavistic reversion to a more fish-like symmetry (Beverdam et al., 2002; Depew et al., 2002). However, since fish have cartilage rods in both the upper (palatoquadrate) and lower jaws (Meckel's cartilage) and the knockout mice lack cartilage in either jaw, this interpretation is inaccurate. The *Dlx5/6* null mice may be telling us something different about evolution. Rather, that mammals cannot be made to resemble fish due to a recently evolved distinctive maxillary region, whose bony derivatives replace the palatoquadrate. It would take the induction of a cartilage rod in the maxilla in order for mammals to revert to a more primitive gnathostome. While there many examples of ectopic cartilage in a proximal position near the jaw joint (Smith and Schneider, 1998), we are not aware of a situation where a cartilage rod replaces the maxillary bones.

In summary, our data show that from the time the first pharyngeal arch forms at stage 13, neural crest-derived mesenchymal cells in the head and first pharyngeal arch prefigure their later positions in the facial prominences. Cells that fill the maxillary prominence are already located in the maxillary condensation and are presumably waiting for local growth cues to begin differential proliferation. Our data support the concept that the maxillary prominence is not a derivative of the first pharyngeal arch. Moreover, since the major derivatives of the first visceral arch are the mandible and joint, it is entirely appropriate to call the first arch, the mandibular arch.

Acknowledgments

We gratefully acknowledge M. Bronner-Fraser and R. Cerny for valuable discussions and for sharing unpublished data with us. We thank E. Humphries and S.W. Cho for providing technical support. JMR is funded by grants from the Canadian Institutes of Health and a Distinguished Scholar award from the Michael Smith Foundation for Health Research. S-HL is funded by grant number R13-2003-13 from the Medical Science and Engineering Research Program of the Korean Science and Engineering Foundation. O. Bédard was funded through a North Fellowship.

References

Ashique, A.M., Fu, K., Richman, J.M., 2002a. Endogenous bone morphogenetic proteins regulate outgrowth and epithelial survival during avian lip fusion. Development 129, 4647–4660.

Ashique, A.M., Fu, K., Richman, J.M., 2002b. Signalling via type IA and type IB bone morphogenetic protein receptors (BMPR) regulates intramembranous bone formation, chondrogenesis and feather formation in the chicken embryo. Int. J. Dev. Biol. 46, 243–253.

Baker, C.V., Bronner-Fraser, M., Le Douarin, N.M., Teillet, M.A., 1997. Early- and late-migrating cranial neural crest cell populations have equivalent developmental potential in vivo. Development 124, 3077–3087.

Barlow, A.J., Francis-West, P.H., 1997. Ectopic application of recombinant BMP-2 and BMP-4 can change patterning of developing chick facial primordia. Development 124, 391–398.

Barlow, A.J., Bogardi, J.P., Ladher, R., Francis-West, P.H., 1999. Expression of chick Barx-1 and its differential regulation by FGF-8 and BMP signaling in the maxillary primordia. Dev. Dyn. 214, 291–302.

Bellairs, A.D.A., 1958. The early development of the interorbital septum and the fate of the anterior orbital cartilages in birds. J. Embryol. Exp. Morphol. 6, 68–85.

Bermis, W.E., Grande, L., 1992. Early development of the actinopterygian head. 1. External development and staging of the paddlefish *polyodon spatula*. J. Morphol. 213, 47–83.

Beverdam, A., Merlo, G.R., Paleari, L., Mantero, S., Genova, F., Barbieri, O., Janvier, P., Levi, G., 2002. Jaw transformation with gain of symmetry after Dlx5/Dlx6 inactivation: Mirror of the past? Genesis 34, 221–227.

Cerny, R., Lwigale, P., Ericsson, R., Meulemans, D., Epperlein, H.-H., Bronner-Fraser, M., 2004a. Mandibular arch morphogenesis and the origin of jaws: new interpretation of "maxillary" and "mandibular". Dev. Biol. (in press).

Cerny, R., Meulemans, D., Berger, J., Wilsch-Brauninger, M., Kurth, T., Bronner-Fraser, M., Epperlein, H.H., 2004b. Combined intrinsic and extrinsic influences pattern cranial neural crest migration and pharyngeal arch morphogenesis in axolotl. Dev. Biol. 266, 252–269.

Couly, G.F., Coltey, P.M., Le Douarin, N.M., 1993. The triple origin of skull in higher vertebrates: a study in quail-chick chimeras. Development 117, 409–429.

Cubbage, C.C., Mabee, P.M., 1996. Development of the cranium and paired fins in the zebrafish *Danio rerio* (Ostariophysi Cyprinidae). J. Morphol. 229, 121–160.

de Beer, G.R., 1931. On the nature of the trabecula cranii. Q. J. Microsc. Sci. 74, 701–731.

de Beer, G.R., 1937. The Development of the Vertebrate Skull. Oxford University Press, Oxford.

Depew, M.J., Lufkin, T., Rubenstein, J.L., 2002. Specification of jaw subdivisions by Dlx genes. Science 298, 381–385.

Francis-West, P.H., Tatla, T., Brickell, P.M., 1994. Expression patterns of the bone morphogenetic protein genes Bmp-4 and Bmp-2 in the developing chick face suggest a role in outgrowth of the primordia. Dev. Dyn. 201, 168–178.

Francis-West, P.H., Robson, L., Evans, D.J., 2003. Craniofacial development: the tissue and molecular interactions that control development of the head. Adv. Anat. Embryol. Cell Biol. 169, 1–138.

Gendron-Maguire, M., Mallo, M., Zhang, M., Gridley, T., 1993. Hoxa-2 mutant mice exhibit homeotic transformation of skeletal elements derived from cranial neural crest. Cell 75, 1317–1331.

Haeckel, E.H.P.A., 1886. The Evolution of Man. A Popular Exposition of The Principal Points of Human Ontogeny and Phylogeny. D. Appleton and Co, New York, NY.

Hamburger, V., Hamilton, H., 1951. A series of normal stages in the development of the chick embryo. J. Morphol. 88, 49–92.

Janvier, P., 1996. Early Vertebrates. Clarendon Press, Oxford.

Kontges, G., Lumsden, A., 1996. Rhombencephalic neural crest segmentation is preserved throughout craniofacial ontogeny. Development 122, 3229–3242.

Lee, S.H., Fu, K.K., Hui, J.N., Richman, J.M., 2001. Noggin and retinoic acid transform the identity of avian facial prominences. Nature 414, 909–912.

MacDonald, M.E., Abbott, U.K., Richman, J.M., 2004. Upper beak truncation in chicken embryos with the cleft primary palate mutation is due to an epithelial defect in the frontonasal mass. Dev. Dyn. 230, 335–349.

McCann, J.P., Owens, P.D., Wilson, D.J., 1991. Chick frontonasal process excision significantly affects mid-facial development. Anat. Embryol. (Berl) 184, 171–178.

McGonnell, I.M., Clarke, J.D., Tickle, C., 1998. Fate map of the developing chick face: analysis of expansion of facial primordia and establishment of the primary palate. Dev. Dyn. 212, 102–118.

Moore, K., Persaud, T.V.N., 2003. Before We are Born: Essentials of Embryology and Birth Defects. Saunders, Philadelphia.

Nelson, O.E., 1953. Comparative Embryology of the Vertebrates. Blakiston Co, New York.

Plant, M.R., MacDonald, M.E., Grad, L.I., Ritchie, S.J., Richman, J.M., 2000. Locally released retinoic acid repatterns the first branchial arch cartilages in vivo. Dev. Biol. 222, 12–26.

Richman, J.M., Lee, S.H., 2003. About face: signals and genes controlling jaw patterning and identity in vertebrates. BioEssays 25, 554–568.

Richman, J.M., Tickle, C., 1989. Epithelia are interchangeable between facial primordia of chick embryos and morphogenesis is controlled by the mesenchyme. Dev. Biol. 136, 201–210.

Richman, J.M., Herbert, M., Matovinovic, E., Walin, J., 1997. Effect of fibroblast growth factors on outgrowth of facial mesenchyme. Dev. Biol. 189, 135–147.

Rijli, F.M., Mark, M., Lakkaraju, S., Dierich, A., Dolle, P., Chambon, P., 1993. A homeotic transformation is generated in the rostral branchial region of the head by disruption of Hoxa-2, which acts as a selector gene. Cell 75, 1333–1349.

Rowe, A., Richman, J.M., Brickell, P.M., 1991. Retinoic acid treatment alters the distribution of retinoic acid receptor-beta transcripts in the embryonic chick face. Development 111, 1007–1016.

Rowe, A., Richman, J.M., Brickell, P.M., 1992. Development of the spatial pattern of retinoic acid receptor-beta transcripts in embryonic chick facial primordia. Development 114, 805–813.

Shen, H., Wilke, T., Ashique, A.M., Narvey, M., Zerucha, T., Savino, E., Williams, T., Richman, J.M., 1997. Chicken transcription factor AP-2: cloning, expression and its role in outgrowth of facial prominences and limb buds. Dev. Biol. 188, 248–266.

Shigetani, Y., Nobusada, Y., Kuratani, S., 2000. Ectodermally derived FGF8 defines the maxillomandibular region in the early chick embryo: epithelial–mesenchymal interactions in the specification of the craniofacial ectomesenchyme. Dev. Biol. 228, 73–85.

Shigetani, Y., Sugahara, F., Kawakami, Y., Murakami, Y., Hirano, S., Kuratani, S., 2002. Heterotopic shift of epithelial–mesenchymal interactions in vertebrate jaw evolution. Science 296, 1316–1319.

Smith, K.K., Schneider, R.A., 1998. Have gene knockouts caused evolutionary reversals in the mammalian first arch? BioEssays 20, 245–255.

Sperber, G.H., 2001. Craniofacial Development. B.C. Decker, Hamilton, Ontario.

Wilson, J., Tucker, A.S., 2004. Fgf and Bmp signals repress the expression of Bapx1 in the mandibular mesenchyme and control the position of the developing jaw joint. Dev. Biol. 266, 138–150.

Yee, G.W., Abbott, U.K., 1978. Facial development in normal and mutant chick embryos: I. Scanning electron microscopy of primary palate formation. J. Exp. Zool. 206, 307–321.